Polish Society of Composite Materials
Polskie Towarzystwo Materiałów Kompozytowych

24: 1 (2024) 9-16

COMPOSITES THEORY AND PRACTICE

ISSN (online): 2299-128X

Dharmeswar Dash[1]*, Devarasiddappa Devarajaiah[2], Santosh Kumar Dash[1], Sutanu Samanta[3], Ram Naresh Rai[4]

[1] GKCIET, Department of Mechanical Engineering, Malda, West Bengal - 732141, India
[2] Rajiv Gandhi Govt. Polytechnic College, Itanagar, Arunachal Pradesh - 791113, India
[3] NERIST, Department of Mechanical Engineering, Arunachal Pradesh - 791109, India
[4] NIT, Department of Production Engineering, Agartala, Tripura - 799046, India
**Corresponding author: E-mail: dharmeswar.bulu@gmail.com*

Received (Otrzymano) 14.07.2023

EXPERIMENTAL INVESTIGATION AND MACHINING ANALYSIS OF Mg/TiC COMPOSITES DURING EDM

https://doi.org/10.62753/ctp.2024.02.1.1

Electrical discharge machining (EDM) is one of the prominent non-conventional machining processes used to machine metal matrix composites. Mg/TiC composites are found in many industrial applications and conventional machining of the same is highly challenging. This paper aims to study the machinability analysis of Mg/TiC composites using EDM with pulse-on time (T_{on}), pulse-off time (T_{off}) and input current (I) as the process variables with the material removal rate (MRR) and surface roughness (SR) as the performance measures. Stir cast Mg-alloy reinforced with TiC (0, 5, 10, 15 and 20) by weight was used as the workpiece. The EDM experiments were conducted as per L_{25} orthogonal array (OA) and the results were analyzed to study the effect of the process variables on MRR and SR. The parametric study showed that SR increases linearly with T_{on} and is attributed to larger craters produced at a higher pulse energy. MRR was also observed to grows with the rise in T_{on} as more material melts due to high-intensity pulses. As per the ANOVA results, T_{on} was found to be the most influential process variable affecting SR and MRR with a 79% and 34% contribution, respectively. Surface morphology investigations using SEM micrographs revealed the presence of globules and sphere-shaped metal deposits and were found responsible for increased SR.

Keywords: **magnesium alloy, TiC, electrical discharge machining, surface quality, material removal rate, surface roughness, analysis of variance**

NOMENCLATURE

MMCs	Metal matrix composites
NTM	Non-traditional machining
MRR	Material removal rate
TWR	Tool wear rate
EDM	Electrical discharge machining
OA	Orthogonal array
NC	Numerical control
ANOVA	Analysis of variance
DOC	Depth of cut
DOE	Design of experiment
SCD	Surface crack density
ROC	Radial over-cut
GRA	Gray relational analysis
MCV	Machine control variables
T-GRA	Taguchi-Gray relational analysis
WEDM	Wire electrical discharge machining
FGAMCs	Functionally graded Al matrix composites
SEM	Scanning electron microscope
OC	Overcut
SR	Surface roughness
EDMed	Electrical discharge machined
RSM	Response surface methodology
CSD	Central composite design

INTRODUCTION

Conventional metals, as we knew them, could not meet the demands for extreme properties that complex operating conditions demanded. One such material is the metal matrix composite. Machining such a high--strength, heat-resistant material into precise shapes takes too long and is often impossible. In-order to meet these requirements various non-traditional machining techniques have emerged out of which EDM is the most extensively used NTM method.

Rengasamy et al. [1] examined the impact of input variables i.e., current, pulse-on time, and pulse-off time on EDM machining of Al 4032 composite reinforced with ZrB_2 and TiB_2 in various wt.% (0, 2, 4, 6, 8) to determine the output responses such as MRR, TWR and DOC. To minimize the number of experiments, designed the experiments according to Taguchi L_{25} OA based on the chosen input variables. Sahani et al. [2] investigated how the changes in the input parameters such as input current (I), voltage (v), and pulse-on time (T_{on}) affect MRR. They came to the conclusion that when the voltage is increased, MRR grows nonlinearly. MRR grows to a certain point when the pulse-on time and current are increased, then declines. Khundrakpam et al. [3] explored the effect of the machine input parameters and tool rotating speed on the SR values of EN-8 workpieces with copper as the electrode by means of NC EDM. The ANOVA results indicated that the input current (I) was more significant, followed by pulse-on time (T_{on}) whereas the rest of the parameters were found not to be significant. Baraskar et al. [4] utilized the machining parameters such as T_{on}, T_{off}, and I using RSM to develop analytical models for MRR and SR for DOE and multi-linear regression analysis techniques. A multi-objective optimization method was utilized to determine the solution to maximize MRR and reduce SR. Mohanty et al. [5] studied the effect of the peak current (I_p), duty factor (T_{au}), and pulse-on duration (T_{on}) on the machining of Inconel alloy. I_p was determined to be the main influencing element for MRR, SR, and ROC, whereas T_{on} was responsible for SCD. Kumar et al. [6] investigated the machining of AISI420 stainless steel utilizing die-sinking EDM with a copper electrode. The T-GRA methodology has been clearly proven to significantly improve the performance parameters in the DS-EDM method. Kumar et al. [7] investigated the effect of the WEDM parameters on the surface roughness (R_a) during the machining of SiC-reinforced Al MMC. With an increasing pulse-on time and peak current, the thickness of the recast layer grows. Nadupuru et al. [8] investigated how the input process variables were affected with or without the use of a magnet during the EDM machining of Inconel 718 material. Uthayakumar et al. [9] reported that the pulse current majorly contributed to the output performance, followed by the zone position and pulse-on time while machining FGAMCs by means of EDM. Mahanta et al. [10] investigated the EDM of Al7075-B_4C-fly ash hybrid MMCs. MRR, and TWR were the performance indicators whereas V, I, T_{on} and T_{off} were the input parameters. It was discovered that I is the most influencing factor followed by T_{on}.

Kandpal et al. [11] used EDM to evaluate the machining features such as MRR, TWR, SR, and OC, as well as the surface topography of the drilled holes (EDM) at different setting of peak current (I_p), pulse-on time (T_{on}), duty factor (DF). According to the results, increasing T_{on} and I_p rises MRR, TWR, the overcut, and SR. However, the duty factor has a smaller impact on these responses. Pugazhenthi et al. [12] investigated the machining parameter and morphology of a 10 vol.% Al_2O_3/Al MMC. It was observed that the pulse-on time has a greater influence on the recast layer thickness followed by the current. Natarajan et al. [13] investigated the EDM of Al7075-B_4C-fly ash hybrid MMCs. It was also discovered that the input current was the most influencing factor followed by pulse-on time.

Dash et al. [14] examined the response of SR and MRR to EDM machining by using both the experimental and Taguchi methods. Additionally, it was noted that the experimentally determined MRR and SR results match the predicted MRR and SR values obtained by the Taguchi method.

Lakshmanan et al. [15] examined how the different input data affected the EDM process of a Mg/SiC_P-fly ash hybrid MMC. The ANOVA results indicate that the applied current and pulse-on time are the two key variables that affect MRR. The parametric study showed that MRR increases with the rise in the applied current, pulse-on time, and pulse-off time. Praveen et al. [16] focused on the influence of the WEDM parameters on the MRR and SR of an AA7075/6 wt.% nickel-coated Al_2O_3 composite. Utilizing GRA in conjunction with principal component analysis (PCA), the best combinations of pulse-on time, pulse-off time, and peak current were found to increase MRR and reduce SR. Shyn et al. [17] focused on the EDM machining of an A6061/ 6%B_4C MMC. The design of the input process parameters based on the CSD, and RSM was used to optimize them. The ANOVA results were utilized to determine the highest MRR, lowest SR, and lowest EWR, which were then examined using the RSM. The optimized results demonstrated improvement over the results that were projected.

Relatively little research on the characterization of EDM machining on Mg/TiC materials with a wide range of TiC reinforcement has been reported by the previous authors. The machinability of Mg/TiC composites was investigated using a servo-controlled EDM device with copper (99% unadulterated) as the electrode material. The investigation showed how the EDM input parameters (the pulse-on time (T_{on}), pulse-off time (T_{off}), and input current (I)) affects of MRR and SR of Mg/TiC MMCs. To further illustrate the statistical relevance of the process factors on the MRR and SR of the Mg/TiC composites, ANOVA soft computing analysis was conducted. Using SEM, analysis of the EDMed surface morphology of the Mg/TiC MMC was conducted in order to assess the quality of the machined surface.

EXPERIMENTAL DETAILS

Materials and machining in EDM

The matrix material for the composite was taken as magnesium alloy AZ91D (a high-purity version of the magnesium alloy) and TiC as the reinforcing material. The average particle size of the TiC powder is 22 μm. The raw materials for the composites were melted in a vertical bottom pouring induction furnace and poured into a 10 × 10 cm rectangular sand mold. The detailed synthesis process is well explained by Dash et al. [18]. Five different compositions of Mg/TiC MMC were synthesized by reinforcing TiC varied with 0, 5, 10, 15, and 20 wt.% in Mg alloy.

The machinability characteristics of the composites were obtained by a spark EDM (SPARKONIX MOS 25 A).

In this process, the workpiece is held in a work-holding device and the tool (copper electrode) is held in the tool holder. A typical EDM setup and copper electrode material is shown in Figures 1 and 2, respectively.

The shape of the electrode is square and made of copper because of its wide availability, low cost, better machinability and ability to produce a better surface finish on the workpieces, and a low wear ratio. To induce spark between tool and workpiece kerosene was used as conducting dielectric fluid [1, 19]. The workpiece and the tool surface are submerged in the dielectric fluid because the dielectric serves some important functions, i.e., a complete electrical circuit, it cools down the tool and workpiece, and cleans the debris at the machining zone. The most important and widely used machine input parameters are taken as the pulse-on time (T_{on}: 21, 50, 100, 150, 200 µs), pulse-off time (T_{off}: 11, 20, 30, 40, 75 µs), and current (I: 4, 5, 6, 7, 8 A).

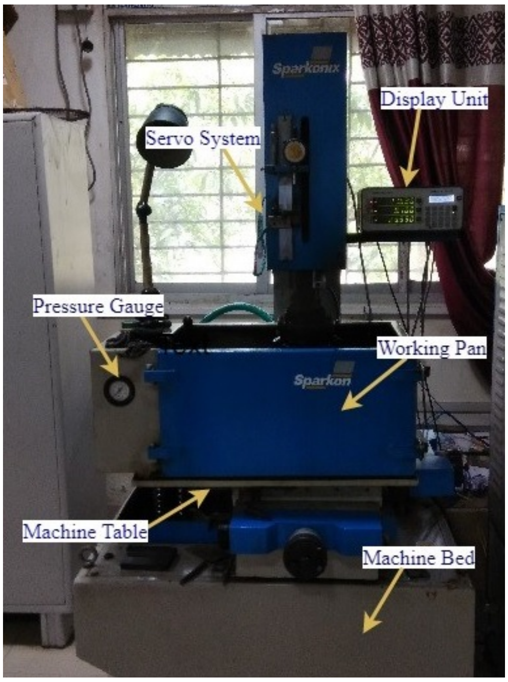

Fig. 1. Typical EDM set-up

Fig. 2. Copper electrode (ratio: 1:1, size: 18.72 mm x 18.72 mm)

To reduce the number of experiments and obtain reliable results, it is imperative to use a suitable design of experiments. Accordingly, 25 experiments were selected as per L_{25} OA. The electrode used in the experiments had a negative polarity and the workpiece a positive one. Whenever the suitable input parameters are supplied a spark is produced in the gap (0.02 to 0.05 mm) between the tool and workpiece surfaces (which is the shortest distance between them). As a result of the spark, heat is generated at the workpiece surface which melts the workpiece material during the pulse-on time and a pressurized flushing system (side flushing at a pressure of 15 kg/cm^2) is employed during the pulse-off time (the time expressed in microseconds between the two pulses on time) to remove eroded particles from the sparking zone. After each operation, the spark gap was maintained by a servo control system.

Factors affecting MRR and SR

MRR can be calculated as the difference in the weight of the workpiece before and after machining divided by the machining time [19]. Over an 8 mm machining length, SR was measured using a Tylor Hobson 2D profilometer. The MRR [g/min] and SR [µm] values obtained during the experimental work are presented in Table 1. For Experiment 21, where the input parameters are 15 wt.% TiC composites, T_{on}: 200 µs, T_{off}: 11 µs, and I: 8 A, the highest MRR was calculated to be 0.1379 (g/min).

TABLE 1. **Input/output parameters of L_{25} orthogonal array**

Sample	**wt.% of TiC**	**Input parameters**			**Output parameters**	
		Current I [A]	**Pulse-on time T_{on} [µs]**	**Pulse-off time T_{off} [µs]**	**SR [µm]**	**MRR [g/min]**
1	0	4	21	11	3.0914	0.005333
2	5	5	21	20	2.4822	0.006053
3	10	6	21	30	3.5303	0.0092
4	15	7	21	40	4.1374	0.015205
5	20	8	21	75	3.3784	0.005667
6	10	5	50	11	2.8032	0.02561
7	15	6	50	20	3.0625	0.031818
8	20	7	50	30	3.1907	0.024955
9	0	8	50	40	3.3981	0.035735
10	5	4	50	75	2.6876	0.006905
11	20	6	100	11	3.8139	0.0375
12	0	7	100	20	3.5343	0.054587
13	5	8	100	30	3.73	0.065375
14	10	4	100	40	2.6055	0.018097
15	15	5	100	75	3.3314	0.017572
16	5	7	150	11	3.1987	0.059655
17	10	8	150	20	5.9841	0.07027
18	15	4	150	30	4.2851	0.028671
19	20	5	150	40	4.3227	0.036364
20	0	6	150	75	4.8483	0.036087
21	15	8	200	11	6.1176	0.1379
22	20	4	200	20	5.0216	0.02623
23	0	5	200	30	6.1982	0.03105
24	5	6	200	40	6.5592	0.047111
25	10	7	200	75	6.5741	0.029872

The smallest MRR was measured in Experiment 1, which was 0.005333 g/min, i.e., 0 wt.% TiC particles, T_{on}: 21 µs, T_{off}: 11 µs, and I: 4 A.

The parameter setting corresponds to Experiment 2 (WP = 5 wt.%, T_{on} = 21 µs, T_{off} = 20 µs, and I = 5 A), which yields the lowest surface roughness value of R_a = 2.4822 µm.

The highest surface roughness of R_a = 6.5741 µm was recorded at cutting conditions corresponding to Experiment 25 (WP = 10 wt.%, T_{on} = 200 µs, T_{off} = = 75 µs and I = 7 A). The roughness profiles corresponding to Experiment 2 and 25 are depicted in Figures 3 and 4, respectively.

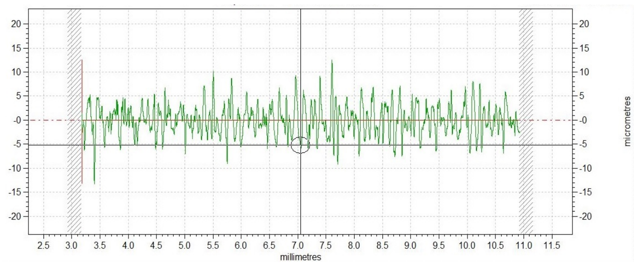

Fig. 3. Roughness profile of machined surface from Experiment 2

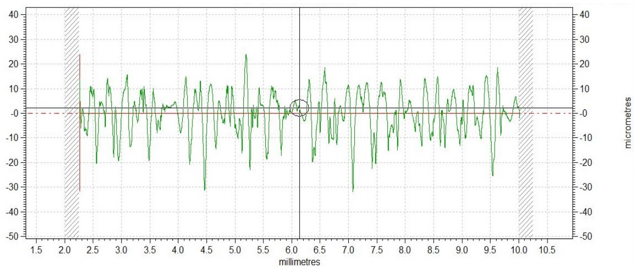

Fig. 4. Roughness profile of machined surface from Experiment 25

ANOVA ANALYSIS FOR MRR AND SR

It is desirable to determine the effect of the most influencing parameter(s) on the response of MRR and SR. The ANOVA statistical technique was used at a 95% confidence level to study the significance of the EDM input parameters on MRR and SR. If the p-value (calculated probability) is less than 0.05, the input process parameter is considered to be significant, otherwise, the parameter is said to be insignificant. For the computational work, MINITAB 17 software was used.

ANOVA analysis for MRR

Table 2 shows the ANOVA results of MRR. The % of the contribution of each input process parameter to the variance in the response variable for MRR is also summarized. The ANOVA results indicate that the pulse-on time (p = 0.014) and current (p = 0.016) have a significant effect on MRR as the obtained p-values are less than the level of significance (0.05). At a 95% confidence level, the impact of TiC weight percentage and pulse-off time on MRR were not statistically significant. The most important process parameter impacting MRR was found to be the pulse-on time (34.48% contribution), followed by current (32.5%). The contribution for the pulse-off time and reinforcement weight percentage was obtained as 15.99% and 6.023% respectively, and they were found to be statistically insignificant. Higher MRR results due to an increment in T_{on} caused a rise in the amount of spark energy and growth in I_p also increased the MRR.

TABLE 2. **MRR ANOVA results**

Source of variance	Sum of squares	DF	Mean sum of squares	F	PC [%]	p-value
TiC [wt.%]	0.00116	4	0.00029	1.1	6.023	0.421
Pulse-on time	0.00664	4	0.00166	6.25	34.48	**0.014**
Pulse-off time	0.00308	4	0.00077	2. 9	15.99	0.093
Current	0.00626	4	0.00156	5.59	32.5	**0.016**
Error	0.00212	8	0.00026		11.01	
Total	0.01926	24			100.00	

ANOVA analysis for SR

Table 3 displays the ANOVA result of SR. Each process parameter's contribution to the variation in the SR response variable was calculated and summarized. Based on the ANOVA results, it can be inferred that the pulse-on time was the most dominant EDM process parameter affecting SR with a 79.12% contribution. Current was established as the second most dominant input variable with a 7.85% contribution, followed by TiC weight percentage (2.69%) and pulse-off time (1.4%).

The obtained p-values from Table 3 indicate that the pulse-on time is statistically significant. Neverthless, the current, pulse-off time and weight percentage imply that the effect of these process parameters on SR is not statistically significant. With an increase in T_{on}, SR of the machined surface rises. With the rise in T_{on} a large amount of molten material was generated and the generated molten metal solidifies at the workpiece surface instead of being removed from the machining zone owing to a high impulsive force.

TABLE 3. **SR ANOVA results**

Source of variance	Sum of squares	DF	Mean sum of squares	F	PC [%]	p-value
TiC [wt.%]	1.0848	4	0.27119	0.60	2.69	0.6727
Pulse-on time	31.9646	4	7.99114	17.71	79.12	**0.0005**
Pulse-off time	0.5675	4	0.14189	0.31	1.40	0.8607
Current	3.172	4	0.79299	1.76	7.85	0.2305
Error	3.6101	8	0.45127		8.94	
Total	40.399	24			100.00	

SURFACE MORPHOLOGY STUDY OF EDMed COMPONENTS

This section presents the surface morphology of the EDMed Mg/TiC samples. Figures 5 and 6 present the SEM micrographs of the Mg/TiC samples obtained after machining under cutting conditions corresponding to Experiments 2 and 25, which have the lowest and highest surface roughness in the entire experimental domain, respectively. In Experiment 25, the pulse-on time was found to be the highest value and as a result, as the spark duration grows, more debris is produced at the machining surface. During the pulse-off time, the difficulty in separating the debris from the machining field may be a consequence of insufficient dielectric pressure. The heated debris persists in the machining zone throughout the short pulse-off time in the machining cycle and is solidified in the form of globules, spherical deposits, micro-cracks etc. [20]. The presence of small black spots on the machined surface is evident as seen in Figure 5. It indicates that debris that is not removed from the working zone by flushing of the dielectric as it remains attached to the workpiece surface. As the pulse-on time grows, large numbers of sparks impinge on the workpiece surface, melting more workpiece material, resulting in the accumulation of debris on the machined surface as evident from the SEM micrograph shown in Figure 6. This in turn results in increased surface roughness.

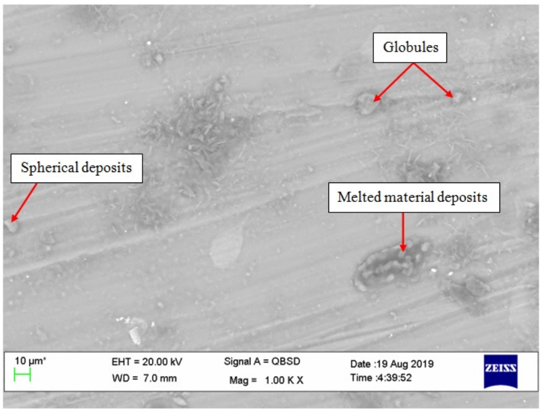

Fig. 5. SEM micrograph of EDMed surface from Experiment 2

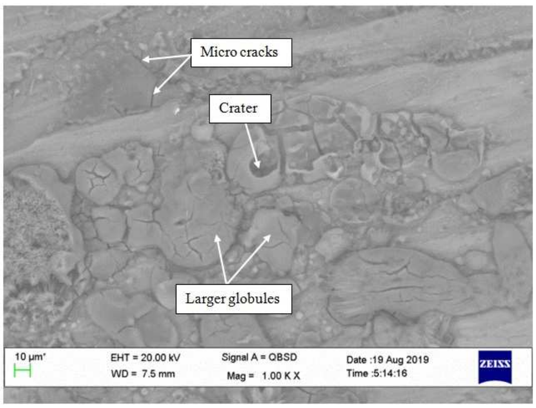

Fig. 6. SEM micrograph of EDMed surface from Experiment 25

PARAMETRIC STUDY OF PERFORMANCE MEASURES

Parametric study of SR

The parametric variation in SR with different EDM input parameters is presented in this section. Figure 7a indicates the variation in the pulse-on time with SR. The values of other process parameters i.e., wt.%, T_{off}, and I are also provided. It can be observed from the parametric graph shown in Figure 7a that in the whole experimental region, SR rises linearly as the pulse-on time increases. The reason is that with the growth in T_{on}, large-size craters are produced because of the higher pulse energy and as a result SR increases [21]. The amount of removed material therefore depends on the crater depth, thereby increasing SR with an increase in crater depth. A similar observation has been attributed by Pradhan and Biswas [22]. Hence, it is preferable to use a low value of T_{on} to minimize SR. The effect of the input current on SR is illustrated in Figure 7b. In the entire experimental domain, it can be seen that SR grows consistently as the input current increases. This is because a rise in current increases the spark energy, leading to larger craters on the workpiece surface. As a result, the machined component has an uneven surface, thereby resulting in greater SR. Annamalai et al. [23] presented a similar observation of the input current with surface roughness variation.

Figure 7c represents the influence of the pulse-off time on SR in the EDM of Mg/TiC MMCs. It was found that an increment in pulse-off time greatly increases SR at all levels. Palanisamy et al. [24] made similar findings in their work. This is because the debris removed from the workpiece is re-solidified on the workpiece surface as the pulse-off time rises rather than being flushed away by the dielectric fluid, resulting in a higher roughness value. The variation in the SR value at different wt.% of TiC reinforcement in MMC is shown in Figure 7d. From the parametric graph, SR is seen to grow with an increase in TiC weight percentage up to 15% and then it decreases.

The rise in SR was observed for all the combinations of input parameters T_{on} - T_{off} - I - WP: 50-40-8-0, 100-30-8-5, 150-20-8-10, 200-11-8-15 except for the combination T_{on} (200 µs) - T_{off} (20 µs) - I (4 A) at 20 wt.% TiC. This can be attributed to the higher value of current (8 A) in all the combinations of input parameters where the surface roughness is higher. As observed from Figure 7b, SR rises as the input current increases in the entire experimental domain. Here, for the given parameter combinations, as the input current is reduced from 8 A to 4 A, the surface roughness also decreases. From the measured SR, it can be concluded that the TiC reinforcement in the magnesium metal matrix significantly increased the machining SR with the rise in reinforcing particles in the magnesium metal matrix [25].

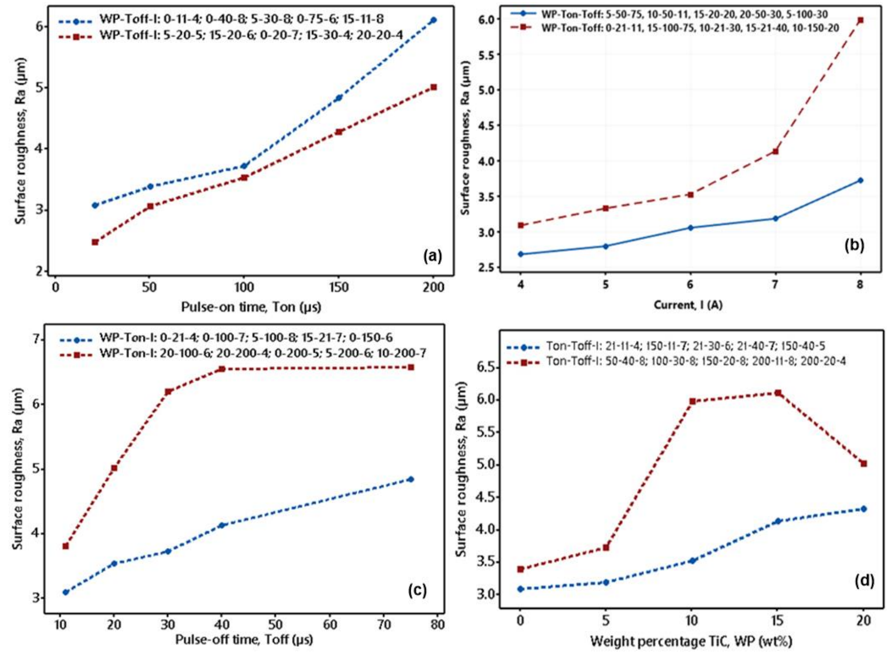

Fig. 7. Parametric variation of SR with: a) pulse-on time, b) current, c) pulse-off time, and d) weight percentage TiC, WP [wt.%]

Parametric study of MRR

Figure 8 shows the variation in MRR with the four process variables considered in this study. The constant values of the other process variables are also shown in the respective graph. The parametric variation in MRR with T_{on} is depicted in Figure 8a. As evident from the parametric graph, MRR grows with an increment in T_{on}, and can be attributed to the increased pulse energy at higher levels of T_{on}. As a result, the workpiece surface is subjected to higher heat, leading to accelerated melting, and hence a higher MRR [26]. Improvement in MRR as the current was increased in the range 4-8 A is also evident in Figure 8b.

This is mainly attributed to localized high energy impulsive sparks impinging on the workpiece surface, resulting in more molten metal, leading to a surge in MRR as the current was varied from lower to higher levels [27]. A similar observation can also be seen in the parametric graphs displayed in Figure 8c. MRR is observed to surge with an increase in T_{off}. This is due to the duration between the two pulses for flushing of the molten metal as T_{off} grew from a lower to higher level, consequently leading to a greater MRR. The weight percentage of TiC also plays a vital role in the enhancement of MRR during EDM of the Mg/TiC composites as seen from the parametric graph depicted in Figure 8d.

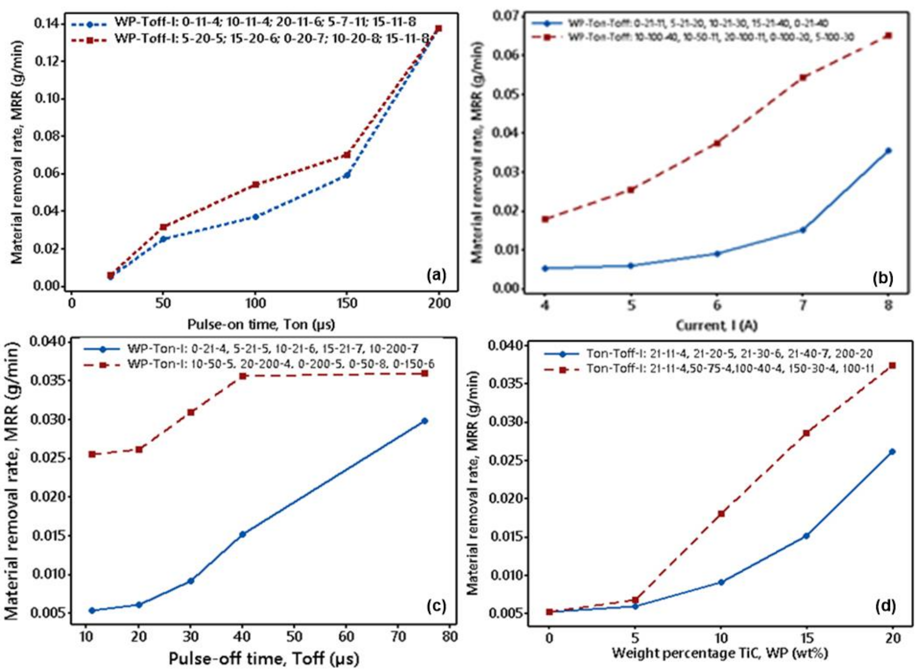

Fig. 8. Parametric variation of MRR with: a) pulse-on time, b) current, c) pulse-off time, and d) weight percentage TiC, WP [wt.%]

CONCLUSION

In this paper, an experimental study and machinability analysis of Mg/TiC composites using the EDM process were presented considering T_{on}, T_{off} and I as the machining parameters to evaluate the two performance measures i.e., MRR and SR. The weight percentage of TiC (0, 5, 10, 20) was also considered as an additional parameter in conducting the EDM experiments. The experimental results were analyzed using ANOVA to determine the influence of the input factors on the responses. The parametric study and SEM micrographs were discussed. The following conclusions were made from the present research work:

1. The experimental results showed that maximum MRR (0.1379 g/min) was obtained at the parameter settings corresponding to Experiment 21 (WP = = 15 wt.%, T_{on} = 200 µs, T_{off} = 11 µs, and I = 8 A) while the lowest SR (2.4822 µm) was achieved at Experiment 2 (WP = 5 wt.%, T_{on} = 21 µs, T_{off} = = 20 µs, and I = 5 A).
2. The ANOVA results showed T_{on} as the most significant factor affecting MRR with a 34.48% contribution followed by I (32.5%), T_{off} (15.99%) and WP (6.02%) respectively. The effects of T_{on} and I were found to be statistically significant at a 95% confidence level.
3. The ANOVA of SR revealed T_{on} as the most dominant EDM process parameter affecting SR with 79.12% contribution and was found statistically significant at a 95% confidence level. The percentage contribution of the other process variables i.e., I (7.85%), WP (2.69%) and T_{off} (1.4%) on SR was observed to be least and statistically insignificant.
4. A steady and gradual increase in SR was observed when T_{on}, T_{off} and I were increased from level 1 to 3. Nevertheless, a sharp increase in SR was evident at higher levels of T_{on} (200 µs) and I (8 A) which can be attributed to large craters on the machined surface due to high energy sparks impinged on the workpiece. Similarly, MRR was observed to increase as T_{on} and I were varied from lower to higher levels. The highest MRR was obtained at higher levels of T_{on} and I as more metal was melted owing to high energy pulses.
5. The SEM micrograph of the composite obtained at WP = 5 wt.%, T_{on} = 21 µs, T_{off} = 20 µs, and I = 5 A corresponding to Experiment 2 showed a comparatively smooth surface with the least surface variation. Some debris and small globules are evident on the machined surface. Nevertheless, the SEM micrograph of the machined component at WP = = 10 wt.%, T_{on} = 200 µs, T_{off} = 75 µs, and I = 7 A (Experiment 25) revealed the presence of large craters and, solidified spherical deposits, leading to an uneven surface and higher SR.

Future scope: The research findings presented in the paper are useful for academicians and research scholars to advance in the area of the non-conventional machining of Mg/TiC composites. The present investigation can be extended by considering other EDM parameters such as the dielectric fluid pressure, different die materials etc. A study of the power consumption as one of the responses can also be explored. Single and multi-response optimization is another promising future scope of work of the present investigation.

Acknowledgements

The authors are grateful to NIT, Agartala for providing the necessary facilities to successfully carry out this work.

REFERENCES

[1] Rengasamy N.V., Rajkumar M., Kumaran S.S., An analysis of mechanical properties and optimization of EDM process parameters of Al 4032 alloy reinforced with Zrb_2 and Tib_2 in-situ composites, Journal of Alloys and Compounds 2016, 662, 325-338.

[2] Sahani O.P., Kumar R., Vashista M., Effect of electro discharge machining process parameters on material removal rate, Journal of Basic and Applied Engineering Research 2014, 1, 17-20.

[3] Khundrakpam N.S., Brar G.S., Deepak D., Grey-Taguchi optimization of near dry EDM process parameters on the surface roughness, Materials Today: Proceedings 2018, 5, 4445-4451.

[4] Baraskar S.S., Banwait S.S., Laroiya S.C., Multi-objective optimization of electrical discharge machining process using a hybrid method, Materials and Manufacturing Processes 2013, 28, 348-354, DOI: 10.1080/10426914.2012.700152.

[5] Mohanty A., Talla G., Gangopadhyay S., Experimental investigation and analysis of EDM characteristics of Inconel 825, Materials and Manufacturing Processes 2014, 29, 540-549, DOI: 10.1080/10426914.2014.901536.

[6] Kumar S., Ghoshal S.K., Arora P.K., Nagdeve L., Multivariable optimization in die-sinking EDM process of AISI420 stainless steel, Materials and Manufacturing Processes 2020, DOI: 10.1080/10426914.2020.1843678.

[7] Kumar H., Manna A., Kumar R., Modeling of process parameters for surface roughness and analysis of machined surface in WEDM of Al/SiC-MMC, Transactions of the Indian Institute of Metals 2018, 71, 1, 231-244, DOI: 10.1007/s12666-017-1159-x.

[8] Nadupuru R., Suman K.N.S., Experimental investigation and evaluation of EDM characteristics of inconel 718 material with and without assistance of magnet, International Journal on Interactive Design and Manufacturing (IJIDeM) 2021, 15, 225-238, DOI: 10.1007/s12008-021-00754-4.

[9] Uthayakumar M., Babu K.V., Kumaran S.T., Kumar S.S., Winowlin J.T., Rajan T.P.D., A study on the machining of Al–SiC functionally graded metal matrix composite using die-sinking EDM, Particulate Science and Technology 2017, DOI: 10.1080/02726351.2017.1346020.

[10] Mahanta S., Chandrasekaran M., Samanta S., RSM modeling and Taguchi analysis of EDM of B_4C and flyash reinforced hybrid nanocomposites, Key Engineering Materials 2019, 801, 227-232.

[11] Kandpal B.C., Kumar J., Singh H., Optimization and characterization of EDM of AA 6061/10%Al_2O_3 AMMC using Taguchi's approach and utility concept, Production & Manufacturing Research 2017, 5, 351-370, DOI: 10.1080/21693277.2017.1389315.

[12] Pugazhenthi R., Sreeram D., Scaria C.T., Anbuchezhiyan G., Nanthakumar P., Effect of process parameters on machining of Al-TiC metal matrix composites using RSM, Materials Today: Proceedings 2021, 46, 9, 3282-3287, DOI: 10.1016/j.matpr.2020.11.357.

[13] Natarajan U., Suganthi X.H., Periyanan P.R., Modeling and multiresponse optimization of quality characteristics for the micro-EDM drilling process, Transactions of the Indian Institute of Metals 2016, 69, 1675-1686, DOI: 10.1007/s12666-016-0828-5.

[14] Dash D., Samanta S., Rai R.N., Flexural, dry sliding wear and machinability (EDM) characteristics of AZ91D/TiC (0, 5, 10, 15, & 20 wt.%) MMCs, Advances in Materials and Processing Technologies 2022, 8, 3, 3344-3362, DOI: 10.1080/2374068X.2021.1949537.

[15] Lakshmanan P., Kumanan G., Arunkumar L., Amith S. C., Experimental investigations of material removal rate on Mg/SiCp-flyash hybrid metal matrix composites by electrical discharge machining, Materials Today: Proceedings 2021, 46, 986-990.

[16] Praveen D.V., Raju M.V.J., Raju D.R., WEDM parametric study of AA7075/6 wt.% Ni-coated Al_2O_3(P) composite miniature gears, Composites Theory and Practice 2023, 23(2), 89-96.

[17] Shyn C.S., Rajesh R., Anand M. Dev., Modeling and prediction of die sinking EDM process parameters for A6061/6%B_4C metal matrix composite material, Materials Today: Proceedings 2021, 42, 677-685.

[18] Dash D., Singh R., Samanta S., Rai R.N., Influence of TiC on microstructure, mechanical and wear properties of magnesium alloy (AZ91D) matrix composites, Journal of Scientific & Industrial Research 2020, 79, 164-169.

[19] Gopalakannan S., Senthilvelan T., Optimization of machining parameters for EDM operations based on central composite design and desirability approach, Journal of Mechanical Science and Technology 2014, 28(3), 1045-1053, DOI: 10.1007/s12206-013-1180-x.

[20] Mohanty A., Talla G., Gangopadhyay S., Experimental investigation and analysis of EDM characteristics of Inconel 825, Materials and Manufacturing Processes 2014, 29, 540-549, DOI: 10.1080/10426914.2014.901536.

[21] Devarasiddappa D., Chandrasekaran M., Arunachalam R., Experimental investigation and parametric optimization for minimizing surface roughness during WEDM of Ti_6Al_4V alloy using modified TLBO algorithm, Journal of the Brazilian Society of Mechanical Sciences and Engineering 2020, 42, 128-145, DOI: 10.1007/s40430-020-2224-7.

[22] Pradhan M.K., Biswas C.K., Effect of process parameters on surface roughness in EDM of tool steel by response surface methodology, International Journal of Precision Technology 2011, 2, 64-80.

[23] Annamalai N., Sivaramakrishnan V., Kumar B.S., Baskar N., Investigation and modeling of electrical discharge machining process parameters for AISI 4340 steel, International Journal of Engineering and Technology (IJET) 2014, 5, 4761-4770.

[24] Palanisamy D., Devaraju A., Manikandan N., Balasubramanian K., Arulkirubakaran D., Experimental investigation and optimization of process parameters in EDM of aluminium metal matrix composites, Materials Today: Proceedings 2020, 22, 525-530, DOI: 10.1016/j.matpr.2019.08.145.

[25] Kumar V., Singh B., Himanshu, Chandel S., Singhal P., Evaluation of EDM characteristics of synthesised AA2024-2 & 3 wt.% SiO_2 metal matrix nanocomposite (MMNC). Materials Today: Proceedings 2020, 26(9), DOI: 10.1016/j.matpr.2020.02.298.

[26] Devarasiddappa D., Chandrasekaran M., Valuation of power consumption and MRR in WEDM of Ti-6Al-4V alloy and its simultaneous optimization for sustainable production, Journal of the Brazilian Society of Mechanical Sciences and Engineering 2018, 40(400), 1-18, DOI: 10.1007/s40430-018-1318-y.

[27] Devarasiddappa D., Chandrasekaran M., Experimental investigation and optimization of sustainable performance measures during WEDM of Ti6Al4V alloy using preference based TLBO algorithm, Materials and Manufacturing Processes 2020, 35(11), 1204-1213. DOI: 10.1080/10426914.2020.1762211.

